# First principles calculations of the structural and electronic properties of the type-I semiconductor clathrate alloys $Ba_8Ga_{16}Si_xGe_{30-x}$ and $Sr_8Ga_{16}Si_xGe_{30-x}$

Emmanuel N. Nenghabi and Charles W. Myles

*Department of Physics, Texas Tech University, Lubbock, Texas 79406-1051, USA*

We studied the structural and electronic properties of some of the Ba and Sr guest-containing type-I semiconductor clathrate alloys $Ba_8Ga_{16}Si_xGe_{30-x}$ and $Sr_8Ga_{16}Si_xGe_{30-x}$ for three values of the Si composition $x$ ($x=0,5,15$). Our calculations are based on the generalized gradient approximation to density functional theory. Starting with the stable structures of the clathrate semiconductors $Ba_8Ga_{16}Ge_{30}$ and $Sr_8Ga_{16}Ge_{30}$ containing no Ga-Ga bonds, we constructed unit cells of $Ba_8Ga_{16}Si_xGe_{30-x}$ and $Sr_8Ga_{16}Si_xGe_{30-x}$ by replacing appropriate numbers of the framework Ge atoms with Si. For the values of the Si composition $x$ that we considered, we found that the fundamental band gap of $Ba_8Ga_{16}Si_xGe_{30-x}$ decreases with increasing $x$. However, we found that the band gap of $Sr_8Ga_{16}Si_xGe_{30-x}$ increases with increasing $x$. Our results also show that several electronic states near the top of the valence band and near the bottom of the conduction band in both materials are modified by the Si $p$ states. The trends in the structural and electronic properties of these materials as $x$ is varied are discussed, and our results are compared to experiment where possible.

PACS number(s): 71.20.Nr, 72.80.Cw

## I. INTRODUCTION

Because of their rich physical properties, materials based on the Ge and Si type-I clathrate structure[1–5] have attracted considerable scientific interest and have resulted in numerous experimental[2,6–9] and theoretical[6,10–12] research studies. These materials are also very interesting technologically because of their promising thermoelectric properties.[13]

The group IV clathrate phases consist of open-framework lattices in which the framework atoms are covalently bonded to each other in fourfold-coordinated $sp^3$ configurations. They are metastable, expanded volume phases of Ge and Si. Ge and Si clathrates are divided into two types based on their crystal structures. A type-I clathrate has a simple cubic lattice containing 46 atoms per unit cell and a type-II material has a face centered cubic lattice containing 136 atoms per cubic unit cell. The lattices of these materials are open-framework structures containing 20-, 24-, and 28-atom cages in which impurity or "guest" atoms can reside. The choice of the guest atoms can be used to tune the properties of the material. Though the local bonding in the clathrates is similar to that in the diamond structure, the clathrates contain pentagonal rings, which make their topology very different from that of the diamond structure.

The pure clathrates (with empty cages) are semiconductors. When the cages contain guests, the guest valence electrons occupy the host conduction bands, and the material becomes metallic. In applications for which a semiconductor is needed, this effect is compensated for by replacing an appropriate number of the host group IV atoms with group III atoms. A compound material such as $Ba_8Ga_{16}Ge_{30}$ is therefore a semiconductor.

Because semiconductor materials have a technological potential for their superior optical and electrical properties, a study of clathrates based on Ge and Si is interesting and potentially important. Recently, Martin *et al.*[13] synthesized type-I semiconductor clathrates based on Ga and Ge with Ba and Sr guests in the cages and with Si substituted for some of the framework atoms. Of course, the properties of these materials strongly depend on the details of their structures. The dynamic disorder of the guest atoms in these materials is thought to be responsible for their low thermal conductivity.[14–16] Static disorder due to the presence of germanium, silicon, and gallium in the framework is also important. In fact, electronic calculations suggest that the gallium distribution and placement in the lattice have a significant effect on the material electronic properties.[11]

In this paper, we present the results of first principles calculations of the structural and electronic properties of the type-I clathrate based materials $Ba_8Ga_{16}Si_xGe_{30-x}$ and $Sr_8Ga_{16}Si_xGe_{30-x}$, where $x$ is the silicon concentration; focusing only on studying the basic structural and electronic properties. Our calculations assumed an ideal $Pm3n$ symmetry for the structure. Among other properties, we present the results of calculations of the fundamental band gap of these clathrates as a function of silicon concentration. For all clathrates considered, except for $Sr_8Ga_{16}Ge_{30}$, we found that the material has an indirect band gap between the Brillouin zone points $\Gamma$ (0, 0, 0) and $M$ (1/2, 1/2, 1/2) and that it ranges from 0.42 to 0.55 eV in $Ba_8Ga_{16}Si_xGe_{30-x}$ and from 0.16 to 0.48 eV in $Sr_8Ga_{16}Si_xGe_{30-x}$. The $Sr_8Ga_{16}Ge_{30}$ material also has an indirect band gap, but it is between the Brillouin zone points $L$ (1/2, 0, 0) and $X$ (1/2, 1/2, 0).

The primary reasons for our interest in $Ba_8Ga_{16}Si_xGe_{30-x}$ and $Sr_8Ga_{16}Si_xGe_{30-x}$ are that some of them have been synthesized in the laboratory and have also been shown to have promising thermoelectric properties.[13] In order to thoroughly understand the thermoelectric and other transport properties of these materials, calculations of the electrical conductivity, the thermal conductivity, and the thermal power are needed. Such calculations would present very challenging problems. Thus, in the present study, we only focused on calculations of some of the structural and electronic properties of these materials. Calculations of the mentioned transport properties of these very interesting materials are beyond the scope of the present study.

## II. COMPUTATIONAL APPROACH

Our calculations are based on the density functional theory and use a plane-wave basis with ultrasoft pseudopotentials. The implementation that we use is the Vienna *ab initio* simulation package (VASP).[17] We used the generalized gradient approximation (GGA) to the exchange correlation functional.[18] The energy cutoff for the plane-wave basis was set to 150 eV and the Brillouin zone integrations were performed over a $4 \times 4 \times 4$ Monkhorst–Pack $k$-space grid.[19] To minimize errors in the calculation of the Hellmann–Feynman forces, the total energy was converged to better than $10^{-6}$ eV. In view of the large clathrate unit cell ($\sim 11$ Å), only a single crystallographic unit cell was employed in the calculations.

Structural optimization was performed by relaxing the internal coordinates to determine the forces and the energies in the lattice. To optimize a structure, a fixed unit cell volume was chosen, and the atomic positions were optimized through a conjugate gradient algorithm by using atomic forces. This process was repeated for several unit cell volumes, from which an equation of state and a global minimum energy were determined. The type-I clathrates have simple cubic lattices, so optimizing the external lattice constant is straightforward. The equilibrium structural parameters, the electronic band structures, and the densities of states were evaluated at the minimum energy configurations.

## III. CLATHRATE STRUCTURE

The type-I clathrate alloys $Ba_8Ga_{16}Si_xGe_{30-x}$ and $Sr_8Ga_{16}Si_xGe_{30-x}$ are simple cubic. These materials are formed by tetrahedral bonding of the Ge, Si, and Ga atoms. Six of the eight Ba or Sr atom guests are located inside the 24-atom cages and the other guests are inside the 20-atom cages. As is well known, the 24-atom cage size is larger than that of the 20-atom cage.

Blake *et al.*[20] showed that the placement of the Ga atoms in the clathrate framework affects the stability of the compound. Since each substitutional Ga has one fewer valence electron than Ge or Si, the Ga concentration and its spatial correlation affect the energetics and the structure of the material. Experimentally, it is known that the Ga occupy non-random framework sites.[21] The guests (Sr and Ba) in these materials are electron donors. Each guest contributes two electrons to the unoccupied conduction bands of $Ga_{16}Ge_{30}$. In the local orbital picture, this process leads to an $sp^3$ bonding structure of the framework atoms. Guest-guest bonding is highly unlikely in these materials because the average distance between guests is about 5.3 Å, which is about five times larger than the ionic radii of Sr (1.13 Å) and Ba (1.35 Å).

### A. $Ba_8Ga_{16}Ge_{30}$ compound

To form the clathrate structures of interest, we begin with the clathrate semiconductor compound $A_8Ga_{16}Ge_{30}$ ($A$ = Sr, Ba). For this material, the number of possible structures that can be generated by placing 16 Ga atoms on the 46 framework sites is huge. Thus, in order to find the most

likely, low energy stable configuration, we performed GGA calculations for various placements of the Ga atoms in the framework. To clearly represent the site occupancies of Ga on the three crystallographic sites of the unit cell, we use Wyckoff's symmetry notations $6c$, $16i$, and $24k$ for the lattice sites. The details of the symmetries of each of these sites are described in detail in Ref. 20. For each calculation, we searched for a low total energy configuration by placing different numbers of the 16 Ga atoms on each symmetry site, by optimizing the geometry, and then by calculating the GGA total energy. These total energies were then compared to each other to find the lowest energy configuration. Of course, for practical reasons, it was possible to consider only a limited number of configurations.

The results of this approach are summarized in Table I. As is shown in Table I, of the structures considered, we find that the configuration with the least number of Ga-Ga bonds and with the fewest Ga atoms on the $16i$ sites is energetically the most stable. The $16i$ sites, with tetrahedral symmetry, are preferentially occupied by group IV atoms and the Ga atoms preferentially occupy either the $6c$ or the $24k$ sites. Obviously, a complete understanding of the energetics of all possible Ga configurations in $A_8Ga_{16}Ge_{30}$ ($A$ = Sr, Ba) cannot be obtained from the limited number of configurations we considered. It is also possible that the total binding energy of the material is a function of both the number of Ga-Ga bonds and of the spatial correlation of the Ga-Ga bonds in the structure. In fact, this trend was observed experimentally.[5] In the first row of Table I, we show that, within the GGA, the energetically most stable Ga configuration for $A_8Ga_{16}Ge_{30}$ ($A$ = Sr, Ba) we found is the one with no Ga-Ga bonds and with 12 Ga atoms on $24k$ sites, with 1 Ga on $16i$ site, and with 3 Ga on $6c$ sites. In each of the calculations for $Ba_8Ga_{16}Si_xGe_{30-x}$ and $Sr_8Ga_{16}Si_xGe_{30-x}$, which are discussed in Sec. IIB, we assumed that the Ga atoms remain on the same lattice sites as they are in the lowest energy configuration of the compound $A_8Ga_{16}Ge_{30}$ ($A$ = Sr, Ba) just discussed.

In this and subsequent calculations, we used the same formalism as that of Blake *et al.*[20] In particular, we pseudopotentials for the guest atoms that include both $s$ and $p$ valence electrons. As is shown in Table I, the energy differences ($\Delta E$) between our results and those of Ref. 20 are 9% or less. We note that the cutoff energies and other simulation parameters may also play a role in producing small energy differences between our results and those of Ref. 20. We also note that all subsequent calculations discussed below for the Si-containing clathrate materials were carried out starting with the lowest energy configurations for $Ba_8Ga_{16}Ge_{30}$ and $Sr_8Ga_{16}Ge_{30}$. Therefore, the higher energy configurations in Table I are not relevant to our primary results. In all the cases discussed in this paper, the total energy was converged to better than $10^{-6}$ eV.

### B. $Ba_8Ga_{16}Si_xGe_{30-x}$ and $Sr_8Ga_{16}Si_xGe_{30-x}$ alloys

Starting with the lowest GGA total energy configuration of $AB_8Ga_{16}Ge_{30}$ ($A$ = Sr, Ba), which was just described, we calculated the electronic and structural properties of the clathrate alloys $Ba_8Ga_{16}Si_xGe_{30-x}$ and $Sr_8Ga_{16}Si_xGe_{30-x}$ by

TABLE I. The GGA total energy for $Ba_8Ga_{16}Ge_{30}$ and $Sr_8Ga_{16}Ge_{30}$ for several different Ga atom locations in the lattice. The first, second, and third columns, respectively, show the number of Ga atoms on the $6c$, $16i$, and $24k$ symmetry sites. We find that the configuration represented by the first row in the table has the lowest GGA total energy. The fifth column shows the differences between our calculated GGA minimum total energies per unit cell and the GGA total energy of the configuration of the first row for the cases. The sixth column shows the total energy differences calculated by others (Ref. 20) for these same configurations.

| $6c$ | $16i$ | $24k$ | Ga-Ga bonds | $\Delta E$, present study (meV) | $\Delta E$, previous study[a] (meV) |
|------|-------|-------|-------------|-------------------------------|-------------------------------------|
| | | | $Ba_8Ga_{16}Ge_{30}$ | | |
| 3 | 1 | 12 | 0 | 0 | 0 |
| 3 | 3 | 10 | 0 | 77.5 | 85 |
| 4 | 2 | 10 | 2 | 259 | 274 |
| 4 | 2 | 10 | 4 | 590 | 544 |
| 5 | 3 | 8 | 4 | 700 | 674 |
| | | | $Sr_8Ga_{16}Ge_{30}$ | | |
| 3 | 1 | 12 | 0 | 0 | 0 |
| 3 | 3 | 10 | 0 | 100 | |
| 4 | 2 | 10 | 2 | 220 | 241 |

[a]Reference 20.

placing varying numbers of Si atoms on the $6c$ and $16i$ sites, as proposed by Martin *et al.*[13] Our calculations show that, for a given Ga distribution, the resulting cell symmetry is reduced from cubic to $C_1$. Despite this, we retained the cubic symmetry in all of our calculations since crystallography "sees" an average cubic unit cell. Reasons for similar assumptions were been justified elsewhere.[20] Further, we found that a cubic distribution of Ga atoms, such as placing all of them on $16i$ sites, results in a higher GGA total energy. We also note that x-ray crystallography for $Sr_8Ga_{16}Ge_{30}$ has shown no detectable distortion in the lattice strains in the framework.[8]

## IV. RESULTS AND DISCUSSION

### A. Structural properties

For a given Si concentration $x$ and for a given placement of the Si atoms on the host framework, we calculated the GGA minimum total energies for $Ba_8Ga_{16}Si_xGe_{30-x}$ and $Sr_8Ga_{16}Si_xGe_{30-x}$ as a function of volume. The calculated total energy vs unit cell volume data were then fitted to the Birch–Murnaghan equation of state.[22] The parameters resulting from this fitting are the minimum binding energy with respect to the free atoms ($E_0$), the corresponding unit cell volume ($V_0$), the bulk modulus ($K$), and the pressure derivative of the bulk modulus, $K' = dK/dP$. As stated above, we assumed that the Ga atoms in these structures remain on the most energetically favorable sites shown in the first row of Table I.

Table II contains our results for the Birch–Murnaghan equation of state parameters at the minimum GGA total energy configuration for $Ba_8Ga_{16}Si_xGe_{30-x}$ and $Sr_8Ga_{16}Si_xGe_{30-x}$. We calculated these parameters for several different Si concentrations $x$ ($x$ is an integer between 0 and 15). However, the results in Table II are shown only for $x = 0$, 5, and 15. As is shown in Table II, the predicted unit cell volume significantly depends on $x$. Our results predict that this volume decreases as $x$ is changed through the sequence $Ba_8Ga_{16}Ge_{30}$, $Ba_8Ga_{16}Si_5Ge_{25}$, and $Ba_8Ga_{16}Si_5Ge_{15}$. We find

TABLE II. Parameters obtained from fitting the calculated GGA total energy at different unit cell volumes to the Birch–Murnaghan equation of state for the clathrate compounds listed. The calculated and the experimental (Refs. 13 and 23) values of the lattice constants are also listed.

| Clathrate | $E_0$ (eV/atom) | $V_0$ ($\text{Å}^3$/atom) | Lattice constant (Å) Theor. | Expt. | $K$ (GPa) | $K' = dK/dP$ |
|-----------|-----------------|---------------------------|------------------------------|-------|-----------|--------------|
| $Ba_8Ga_{16}Ge_{30}$ | −3.98 | 24.41 | 10.97 | 10.76 | 49.12 | 5.3 |
| $Ba_8Ga_{16}Si_5Ge_{25}$ | −4.07 | 23.95 | 10.86 | 10.74 | 55.11 | 5.4 |
| $Ba_8Ga_{16}Si_{15}Ge_1$ | −4.19 | 23.47 | 10.79 | | 59.40 | 4.9 |
| $Sr_8Ga_{16}Ge_{30}$ | −3.89 | 23.78 | 10.87 | 10.74 | 47.0 | 5.5 |
| $Sr_8Ga_{16}Si_5Ge_{25}$ | −3.96 | 23.47 | 10.79 | | 48.20 | 5.5 |
| $Sr_8Ga_{16}Si_{15}Ge_{15}$ | −4.11 | 22.79 | 10.71 | | 53.16 | 4.3 |

a similar trend for the Sr-containing clathrates. This is expected because the bonds between group III atoms and group IV atoms are longer than those between group IV atoms. This might also be a reason for the predicted increased stability of the clathrates as the Si concentration increases. The total binding energies of $Ba_8Ga_{16}Si_xGe_{30-x}$ and $Sr_8Ga_{16}Si_xGe_{30-x}$ are lowered by about 5.6% and 5.7%, respectively, as $x$ is changed from 0 to 15 in each optimized structure.

In these materials, our results also predict that the bulk modulus $K$ is an increasing function of $x$. That is, the larger the Si concentration, the "harder" the material becomes. A qualitative explanation of this phenomenon was proposed by Moriguchi *et al.*,[24] who found that the bulk modulus of a material strongly depends on the number of chemical bonds subjected to a compressive state in a unit volume. Further, the number of such chemical bonds is proportional to the material density. On the other hand, however, we note that San-Miguel *et al.*[25] suggested that, because of charge transfer to the host framework, the relationship between the bulk modulus and the material density is not as simple as this in the case of clathrate structures. Our results further predict that the clathrate materials with Sr guests have smaller lattice constants than those in the corresponding material with Ba guests. This result is consistent with fact that the Sr atom is smaller than the Ba atom.

Table II also shows some of our predictions for the lattice constant for the materials we studied. Where available, experimental results for the lattice constant are also shown in Table II. To our knowledge, those compounds for which no experimental results are listed in Table II have not yet been synthesized in the laboratory. It can be seen in Table II that, where data are available, the predicted and experimental lattice constants are within about 2% of each other.

## B. Electronic properties

Starting with the optimized lattice structure for a fixed Si composition $x$, we calculated the electronic band structures and densities of states for $Ba_8Ga_{16}Si_xGe_{30-x}$ and $Sr_8Ga_{16}Si_xGe_{30-x}$. Figures 1(a)–1(c) and 2(a)–2(c) display our results for the band structures for some of the $x$ values we studied. In those figures, the zero of energy was taken at the top of the valence band. Due to the large number of atoms in the unit cell, the electronic structure is complex, as shown by the large number of bands in the figures.

All of the materials studied here are semiconductors. The total number of valence electrons of the guests in the cages is compensated for by the framework substitutional Ga atoms, which have one fewer electrons than Si and Ge. The precise $k$-point to $k$-point transition for the minimum energy gap in these materials is difficult to accurately determine because the bands are fairly flat, especially around the Fermi level (at the top of the valence band). In all of the structures we considered, except for $Sr_8Ga_{16}Ge_{30}$, the smallest energy gap lies along the $\Gamma$ to $M$ line. We thus conclude that these materials all have indirect band gaps. In $Sr_8Ga_{16}Ge_{30}$, the smallest band gap lies along the $L$ to $X$ line. Our results also show that the band gap is smaller in the compounds with Sr guests than
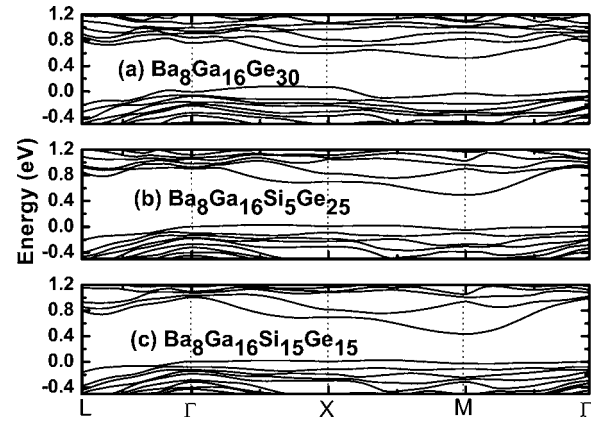


FIG. 1. GGA electronic band structures for (a) $Ba_8Ga_{16}Ge_{30}$, (b) $Ba_8Ga_{16}Si_5Ge_{25}$, and (c) $Ba_8Ga_{16}Si_{15}Ge_{15}$. Each figure displays the predicted energy bands along several symmetry directions of the first Brillouin zone. The Fermi level is set to 0 eV, which is the top of the valence band.

it is in the comparable materials with Ba guests. This is consistent with experiments by Blake *et al.*[26] on these types of clathrate compounds.

Our results predict that the fundamental GGA band gap of $Ba_8Ga_{16}Ge_{30}$ is about 0.55 eV and that it is reduced to about 0.42 eV for $Ba_8Ga_{16}Si_{15}Ge_{15}$. For comparison, Moriguchi *et al.*[24] found that the local density approximation fundamental band gap of the pristine clathrate $Si_{46}$ is 1.11 eV and that for $Ge_{46}$ is 1.31 eV. For the Ba guest-containing materials, we note that, in addition to the results shown for $x=0$, 5, and 15 in Figs. 1(a)–1(c), we also calculated (but not shown) the band structures for $x=3$, 8, and 12. For all values of $x$ that we considered we find that, as the Si concentration $x$ increases, the fundamental band gap slowly decreases. This is in contrast to type-II Si-Ge clathrate alloys, for which others found that the band gap increases with the increasing silicon concentration.[24]

In contrast to the case for $Ba_8Ga_{16}Si_xGe_{30-x}$, our results predict that the band gap for $Sr_8Ga_{16}Si_xGe_{30-x}$ increases with
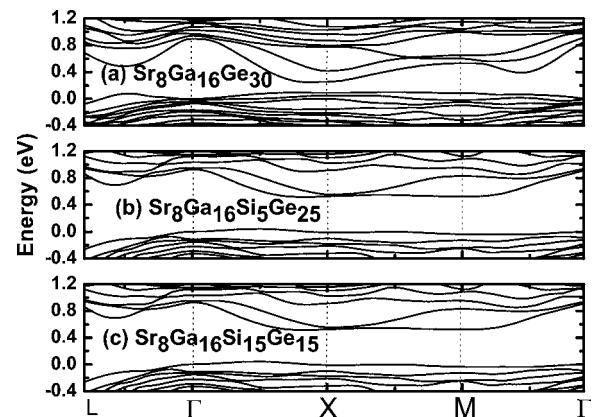


FIG. 2. GGA electronic band structures for (a) $Sr_8Ga_{16}Ge_{30}$, (b) $Sr_8Ga_{16}Si_5Ge_{25}$, and (c) $Sr_8Ga_{16}Si_{15}Ge_{15}$. Each figure displays the predicted energy bands along several symmetry directions of the first Brillouin zone. The Fermi level is set to 0 eV, which is the top of the valence band.

increasing $x$, We find that the gap in $Sr_8Ga_{16}Si_xGe_{30-x}$ changes from about 0.18 eV in $Sr_8Ga_{16}Ge_{30}$ to about 0.48 eV in $Sr_8Ga_{16}Si_{15}Ge_{15}$. Because of the few $x$ values we considered, a definitive conclusion cannot be drawn about the $x$ dependence of the band gap in this material.

A qualitative comparison of the calculated band structures for $Ba_8Ga_{16}Si_xGe_{30-x}$ [Figs. 1(a)–1(c)] and $Sr_8Ga_{16}Si_xGe_{30-x}$ [Figs. 2(a)–2(c)] can, however, be made.

In studies by others[26] on Sr- and Ba-containing Ge-based clathrates without Si in the framework, several reasons were proposed to explain the different behaviors of the fundamental band gaps in the materials with the two types of guests. First, the Sr atom is smaller than the Ba atom and thus can move further away from the cage center. This leads to more anisotropic guest-framework interactions in the Sr-containing clathrates than in the Ba-containing materials.

The calculations of Dong *et al.*[12] for Ga-containing germanium clathrates also confirm this result. They calculated potential energy curves for a single guest atom as a function of small finite displacements of both the Ba and the Sr guest atoms. In these calculations, all other atoms were held fixed in their positions. Within their symmetry assumptions, they found identical potential energy curves for displacements in the $x$ and $y$ directions and a very different curve for displacements in the $z$ direction. A very strong anisotropic behavior of the guests as a function of displacement was found[12] in the $z$ direction, where the metal-host interaction is strongest. This anharmonicity was found to be more pronounced in the Sr compound than in the Ba compound. In the $x$ direction, the potential function for Ba was found to be more harmonic than that for Sr. This is likely because Ba is more massive than Sr. This anisotropic behavior of the guests as a function of displacements was shown to mainly affect the valence bands.[26] These guests vibrate inside the cages with very small energy loss.

Our results also show that the dependence of the lower conduction bands on $x$ is different in $Ba_8Ga_{16}Si_xGe_{30-x}$ than it is in $Sr_8Ga_{16}Si_xGe_{30-x}$. In the Sr-containing materials, the lower conduction bands are much flatter in the X-$M$ region of the Brillouin zone than they are in the Ba-containing materials. This difference can be attributed to the role of the metal guests. These guests donate their electrons to the antibonding states of the host. Since Ba is larger than Sr, it can more easily donate its electrons to the host. For $x=0$, the charge density of the lower conduction was shown[26] to have major contributions from electrons donated from guests in the large host cages. Thus, there is a wave function overlap between the metal guest and the host atoms. This overlap is larger if the guest is close to the host atoms and small if it is further away. This can lead to differences in the hybridized bonding states of the host framework (Ga, Si, and Ge). Reference 26 contains detailed results for the associated charge transfer and its effect on the band structures.

In Table III, we summarize our predicted fundamental band gaps for $Ba_8Ga_{16}Si_xGe_{30-x}$ and $Sr_8Ga_{16}Si_xGe_{30-x}$ for $x$ =0, 5, and 15. It is well known that the GGA underestimates fundamental gaps.[27] Previous work within the GGA by Blake *et al.*[26] predicted that $Ba_8Ga_{16}Ge_{30}$ is a semiconductor while showing that $Sr_8Ga_{16}Ge_{30}$ should be semimetallic.

Of course, the effects of the substitutional Si and Ga atoms in the host Ge framework and the presence of Ba or Sr

TABLE III. Predicted fundamental energy band gaps for the clathrate materials $Ba_8Ga_{16}Si_xGe_{30-x}$ and $Sr_8Ga_{16}Si_xGe_{30-x}$ for various concentrations ($x$) of silicon atoms. The values in parentheses are the predicted energy band gaps from previous work (Ref. 26).

| | GGA fundamental energy band gap (eV) | |
|---|---|---|
| $x$ | $Ba_8Ga_{16}Si_xGe_{30-x}$ | $Sr_8Ga_{16}Si_xGe_{30-x}$ |
| 0 | 0.55 (0.52)[a] | 0.18 (0.2)[a] |
| 5 | 0.49 | 0.47 |
| 15 | 0.42 | 0.48 |

[a]Reference 26.

guests in the cages each will cause modifications in the band structures. Specifically, the effect of each of these atoms in the material is to modify several states near the valence band maxima and the conduction band minima. These effects are illustrated for $Ba_8Ga_{16}Si_5Ge_{25}$ in Fig. 3, which shows the projected electronic state densities for the Si $s$ and Si $p$ orbital states. We found a similar effect for Si in $Sr_8Ga_{16}Si_5Ge_{25}$ (our results for this case are not shown). The contributions of the Ba $s$ (or Sr $s$) electrons to each of these states is negligible and is thus not shown in the figure. As the figure shows, the contributions to the total density of states of the $s$ orbitals near the bottom of the conduction band are very small compared to the contributions of the $p$ orbitals. Of course, the electronic states of the valence electrons are composed of hybrid $sp^3$ orbitals. Therefore, the dominant contributions to these states come from the $p$ orbitals.

Figures 4(a) and 4(b) show our calculated results for the total electronic density of states (DOS) in $Ba_8Ga_{16}Si_xGe_{30-x}$ and $Sr_8Ga_{16}Si_xGe_{30-x}$. In Figs. 4(a) and 4(b), only results for $x=0$ and 5 are shown. Each total density of states has three major regions, an $s$ region, an $sp$ hybrid region, and a $p$ bonding region. As observed in Figs. 4(a) and 4(b), as Si atoms are added to the framework, the Si electronic states couple to the electronic states of $A_8Ga_{16}Ge_{30}$ ($A$=Sr,Ba), modifying the band structure. As expected, we found a similar result for $x=15$.

Figures 4(a) and 4(b) clearly show a small gap in the valence band region at energies of about −0.7 eV. Work by others on the bands in clathrate materials[24] found a similar
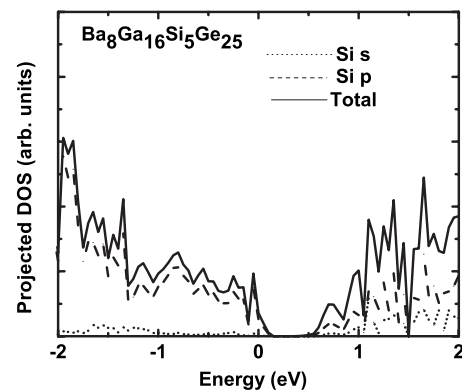


FIG. 3. Projected electronic densities of states for $s$ and $p$ orbitals for Si orbitals in $Ba_8Ga_{16}Si_5Ge_{25}$.
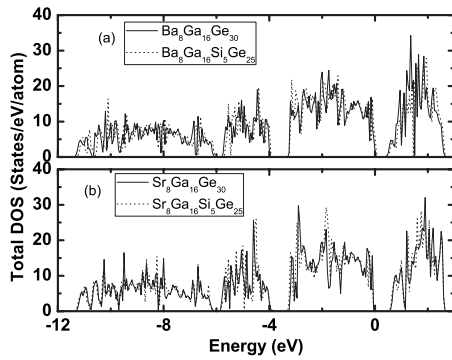
FIG. 4. Total electronic densities of states for (a) $Ba_8Ga_{16}Ge_{30}$ (solid curve) and $Ba_8Ga_{16}Si_5Ge_{25}$ (dotted curve) (b) $Sr_8Ga_{16}Ge_{25}$ (solid curve), and $Sr_8Ga_{16}Si_5Ge_{25}$ (dotted curve).

valence band gap. This gap has been associated with five-ring patterns of the Ge or Si atoms. We note, however, that there were some criticisms on this idea.[28] According to Ref. 29, the small angular distortion of the tetrahedrally bonded framework atoms may also play an important role in producing this gap. In a self-consistent plane-wave calculation, it is impossible to have a value for the valence band maximum on an absolute scale. In the compounds that we studied, the total electronic DOS for each clathrate is qualitatively similar to each of the others.

## V. CONCLUSIONS

We used the GGA to investigate the structural and electronic properties of some of the type-I clathrates of the forms $Ba_8Ga_{16}Si_xGe_{30-x}$ and $Sr_8Ga_{16}Si_xGe_{30-x}$. We presented detailed results for $x=0$, 5, and 15. Where the experimental data exist, the calculated lattice constants are within 2% of the experimental values. By comparing the GGA total energies of various configurations with differing numbers of Ga-Ga bonds in $A_8Ga_{16}Ge_{30}$ ($A=$Sr, Ba), we found that structures with smaller numbers of Ga-Ga bonds yield the lowest total energies. To construct the unit cells for the Ge-Si clathrates, we started with the lowest energy structure for

$A_8Ga_{16}Ge_{30}$ ($A=$Sr, Ba) and replaced varying numbers of Ge atoms with Si. The band structures and the electronic densities of states were calculated for several values of $x$ in $Ba_8Ga_{16}Si_xGe_{30-x}$ and $Sr_8Ga_{16}Si_xGe_{30-x}$. We find that, for all $x$ we considered, these clathrates should have an indirect band gap. The predicted fundamental gaps are in the range 0.42–0.55 eV for $Ba_8Ga_{16}Si_xGe_{30-x}$ and 0.16–0.48 eV in $Sr_8Ga_{16}Si_xGe_{30-x}$. Energy versus displacement curves for the guests, which were obtained by others, are known to predict a large anisotropic behavior for the Sr guests. This is found to severely affect the valence bands. The wave function overlap between the metal guests and host accounts for the differences found in the conduction bands. An analysis of the projected state densities shows that the $p$ states of Si hybridize with those of the framework, which reduces the fundamental band gap of the Ba containing clathrates only.

We hope that our predicted structural and electronic properties for the clathrate alloys $Ba_8Ga_{16}Si_xGe_{30-x}$ and $Sr_8Ga_{16}Si_xGe_{30-x}$ will lead to investigations of the thermoelectric properties of these interesting materials. We further hope that these investigations will provide information about which of these materials will be useful in the search for better thermoelectric materials. Because of the promising thermoelectric properties of these clathrate materials, there is still a need for future calculations of quantities such as the thermal power, the electrical conductivity, and the thermal conductivity. Such calculations are beyond the scope of our work.

[1] B. C. Sales, D. G. Mandrus, and B. C. Chakoumakos, in *Recent Trends in Thermoelectric Materials Research II*, Semiconductors and Semimetals Vol. 70, edited by T. M. Tritt (Academic, San Diego, CA, 2001), p. 1.

[2] B. C. Chakoumakos, B. C. Sales, D. Mandrus, and G. S. Nolas, J. Alloys Compd. **296**, 80 (2000).

[3] B. C. Sales, D. Mandrus, and R. K. Williams, Science **272**, 1325 (1996).

[4] B. C. Sales, B. C. Chakoumakos, D. Mandrus, J. W. Sharp, N. R. Dilley, and M. B. Maple, in *Thermoelectric Materials 1998—The Next Generation Materials for Small-Scale Refrigeration and Power Generation Applications*, MRS Symposium Proceedings No. 545, edited by T. M. Tritt, M. G. Kanatzidis, G. Mahan, and H. B. Lyon, Jr. (Materials Research Society, Pittsburgh, PA,

1998), p. 13.

[5] B. Eisenmann, H. Schäfer, and R. Zakler, J. Less-Common Met. **118**, 43 (1986).

[6] B. B. Iversen, A. E. C. Palmqvist, D. E. Cox, G. S. Nolas, G. D. Stucky, N. P. Blake, and H. Metiu, J. Solid State Chem. **149**, 455 (2000).

[7] G. S. Nolas, J. L. Cohn, G. A. Slack, and S. B. Schujman, Appl. Phys. Lett. **73**, 178 (1998).

[8] G. S. Nolas, T. J. R. Weakley, J. L. Cohn, and R. Sharma, Phys. Rev. B **61**, 3845 (2000).

[9] S. B. Schujman, G. S. Nolas, R. A. Young, C. Lind, A. P. Wilkinson, G. A. Slack, R. Patschke, M. G. Kantzidis, M. Ulutagay, and S. J. Hwu, J. Appl. Phys. **87**, 1529 (2000).

[10] N. P. Blake, L. Möllnitz, G. D. Stucky, and H. Metiu, *18th In-*

*ternational Conference on Thermoelectrics* (IEEE, Piscataway, NJ, 1999), pp. 489–492.

[11] N. P. Blake, L. Möllnitz, G. Kresse, and H. Metiu, J. Chem. Phys. **111**, 3133 (1999).

[12] J. J. Dong, O. F. Sankey, G. K. Ramachandran, and P. F. Mc-Millan, J. Appl. Phys. **87**, 7726 (2000).

[13] J. Martin, S. Erickson, G. S. Nolas, P. Alboni, T. M. Tritt, and J. Yang, J. Appl. Phys. **99**, 044903 (2006).

[14] J. L. Cohn, G. S. Nolas, V. Fessatidis, T. H. Metcalf, and G. A. Slack, Phys. Rev. Lett. **82**, 779 (1999).

[15] B. C. Sales, B. C. Chakoumakos, R. Jin, J. R. Thompson, and D. Mandrus, Phys. Rev. B **63**, 245113 (2001).

[16] B. C. Chakoumakos, B. C. Sales, and D. G. Mandrus, J. Alloys Compd. **322**, 127 (2001).

[17] G. Kresse and J. Furthmuller, Phys. Rev. B **54**, 11169 (1996).

[18] Y. Wang and J. P. Perdew, Phys. Rev. B **44**, 13298 (1991).

[19] H. J. Monkhorst and J. D. Pack, Phys. Rev. B **13**, 5188 (1976).

[20] N. P. Blake, D. Bryan, S. Latturner, L. Møllnitz, G. D. Stucky, and H. Metiu, J. Chem. Phys. **114**, 10063 (2001).

[21] Y. Zhang, P. L. Lee, G. S. Nolas, and A. P. Wilkinson, Appl. Phys. Lett. **80**, 2931 (2002).

[22] The Birch–Murnaghan equation for the energy $E$ as a function of volume $V$ is $E(V) = E_0 + \frac{9}{8} K V_0 [(V_0/V)^{2/3} - 1]^2 \{1 + [4 - K'/2][1 - (V_0/V)^{2/3}]\}$, where $E$ and $E_0$ are the energy and minimum energy, $V$ and $V_0$ are the volume and volume at the minimum energy, and $K$ and $K'$ are the bulk modulus and its pressure derivative.

[23] L. Qiu, I. P. Swainson, G. S. Nolas, and M. A. White, Phys. Rev. B **70**, 035208 (2004).

[24] K. Moriguchi, S. Munetoh, and A. Shintani, Phys. Rev. B **62**, 7138 (2000).

[25] A. San-Miguel, P. Keghelian, X. Blasé, P. Melinon, A. Perez, J. P. Itie, A. Polian, E. Reny, C. Cros, and M. Pouchard, Phys. Rev. Lett. **83**, 5290 (1999).

[26] N. P. Blake, S. Latturner, J. D. Bryan, G. D. Stucky, and H. Metiu, J. Chem. Phys. **115**, 8060 (2001).

[27] J. J. Dong and O. F. Sankey, J. Phys.: Condens. Matter **11**, 6129 (1999).

[28] K. Moriguchi, M. Yonemura, A. Shintani, and S. Yamanaka, Phys. Rev. B **61**, 9859 (2000).

[29] S. Saito and A. Oshiyama, Phys. Rev. B **51**, 2628 (1995).